International Journal of Scientific & Engineering Research, Volume 4, Issue 5, May-2013
ISSN 2229-5518

High Boost Hybrid Transformer DC–DC Converter for Photovoltaic Module Applications

K.Umadevi ,Associate Professor

uma1raj2000@gmail.com

***Abstract*—This paper presents a nonisolated, high boost ratio hy-brid transformer dc–dc converter with applications for low-voltage renewable energy sources. The proposed converter utilizes a hy-brid transformer to transfer the inductive and capacitive energy simultaneously, achieving a high boost ratio with a smaller sized magnetic component. As a result of incorporating the resonant operation mode into the traditional high boost ratio pulsewidth modulation converter, the turn-off loss of the switch is reduced, increasing the efficiency of the converter under all load conditions. The input current ripple and conduction losses are also reduced because of the hybrid linear-sinusoidal input current waveforms. The voltage stresses on the active switch and diodes are maintained at a low level and are independent of the changing input voltage over a wide range as a result of the resonant capacitor transfer-ring energy to the output of the converter. The effectiveness of the proposed converter was experimentally verified using a 220-W prototype circuit. Utilizing an input voltage ranging from 20 to 45 V and a load range of 30–220 W, the experimental results show system of efficiencies greater than 96% with a peak efficiency of 97.4% at 35-V input, 160-W output. Due to the high system effi-ciency and the ability to operate with a wide variable input voltage, the proposed converter is an attractive design for alternative low dc voltage energy sources, such as solar photovoltaic modules and fuel cells.**

***Index Terms*—energy sources with low dc voltage, European union (EU) effi-ciency, high boost ratio dc–dc, high efficiency, hybrid transformer, photovoltaic (PV) module.**

I. INTRODUCTION

Due to the rising costs and limited amount of nonrenew-able energy sources, there is an increasing demand for the utilization of renewable energy sources such as photovoltaic (PV) modules. Integrating the power from the PV module into the existing power distribution infrastructure can be achieved through power conditioning systems (PCS). Typical PCS can be accomplished using a single-stage or a double-stage as shown in Fig. 1. The double-stage PCS consists of a dc–dc conversion stage that is connected to either a low-power individual inverter or a high-power centralized inverter that multiple converters could connect to. The dc–dc conversion stage of the PCS requires a high efficiency, high boost ratio dc– dc converter to increase the low dc input voltage from the PV panel to a higher dc voltage. This voltage has to be higher than the peak output voltage of the dc–ac inverter, nominally in the 380–400 V range. The double-stage design can also suppress ac line double frequency by utilizing the active ripple cancellation technique .

The high boost ratio dc–dc converter for such systems can be isolated or nonisolated however, transformer-isolated converters tend to be less efficient and more expensive due to the increased manufacturing costs. A nonisolated dc–dc converter with a high boost ratio would be advantageous for a two-stage PCS because it can be easily integrated with current PV systems while reducing the cost and maintaining a high system efficiency.

Due to the different output voltages from the PV panel, it would be beneficial to have a system with a high efficiency over the entire PV voltage range to maximize the use of the PV during different operating conditions. Another important function of the DC–DC converter for PV applications is being able to implement maximum power point tracking (MPPT). The ability to implement MPPT for an individual PV panel would ensure that a large cluster of PV could maintain maximum power output from each panel without interfering with the other panels in the system. The major consideration for the main power stage of the converter in being able to implement an accurate MPPT is that the input current ripple of the converter has to be low.

The high boost ratio nonisolated dc–dc converter the uses of coupled-inductor and switched-capacitor are attractive for use in a simple high boost ratio converter due to the fact that only a single low voltage active switch is required . The reason that the primary side active switches of the high boost ratio converters have low voltage stress is because of the transformer effect from the coupled-inductors .Since there is a low voltage stress on the active switch, the circuits can then use low voltage MOSFETs that generally have a low Rds(on) and smaller switching periods, decreasing both the conduction and switching losses. An earlier paper on high boost ratio nonisolated dc–dc converter presented a clamp-mode couple-inductor buck–boost converter. The converter's leakage energy from the coupled-inductor was recycled reducing the losses of the system. The output diode stress for this converter was similar to that of a traditional

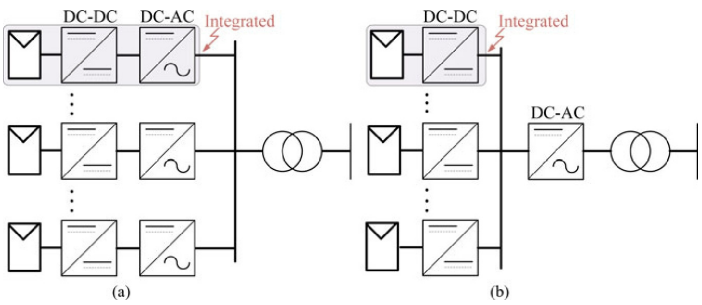

Fig. 1. Typical double-stage PCS architectures with high boost ratio dc–dc converters and PWM dc–ac inverters for PV applications. (a) Two-state PV module integrated microinverter. (b) Parallal PV module integrated microconverter with centralized inverter

Fig. 2. High step-up dc–dc converters using coupled-inductor and switched-capacitor techniques. (a) High-step coupled-indcutor roboost dc-dc converter. (b) High step-up dc-dc converter with coupled-inductor and switched-capacitor.

flyback converter, i.e., higher than the output dc bus voltage. Another drawback of the converter was that there was a high-input current ripple due to the fact that there was no direct energy transfer path when the MOSFET was OFF. Further improvements in increasing the boost ratio of a simple dc–dc converter were accomplished by combining a boost converter with a flyback converter as shown in Fig. 2(a). The boost ratio was improved as a result of the outputs of the boost converter and flyback converter being connected in series. By adding a switched-capacitor in series with the energy transformer path, a new improved high boost ratio dc–dc converter with coupled-inductor and switched-capacitor, as shown in Fig. 2(b). With the switched-capacitor inserted between the primary side and secondary side of the coupled-inductor, the boost ratio was increased and the output diode voltage stress was reduced closer to that of the output dc bus voltage. Light load efficiency of the converter is also reduced because switching losses were more dominant under light load conditions.

In this paper, a high boost ratio dc–dc converter with hybrid transformer is presented to achieve high system level efficiency over wide input voltage and output power ranges. By adding a small resonant inductor and reducing the capacitance of the switched-capacitor in the energy transfer path, a hybrid operation mode , which combines pulsewidth modulation (PWM) and resonant power conversions, is introduced in the proposed high boost ratio dc–dc converter. The inductive and capacitive energy can be transferred simultaneously to the high-voltage dc bus increasing the total power delivered decreasing the losses in the circuit. As a result of the energy transferred through the hybrid transformer that combines the modes where the transformer operates under normal conditions and where it operates as a coupled-inductor, the magnetic core can be used more effectively and smaller magnetics can be used. The con-tinuous input current of the converter causes a smaller current ripple than that of previous high boost ratio converter topolo-gies that used coupled-inductors. The lower input current ripple is useful in that the input capacitance can be reduced and it is easier to implement a more accurate MPPT for PV modules. The conduction losses in the transformer are greatly reduced because of the reduced input current RMS value through the primary side. The voltage stress of the active switch is always at a low voltage level and independent of the input voltages. Due to the introduction of the resonant portion of the current, the turn-off current of the active switch is reduced. As a result of the decreased RMS current value and smaller turn-off current of the active switch, high efficiency

can be maintained at light output power level and low-input voltage operation. Because of the resonant capacitor transferring energy to the output of the converter, all the voltage stresses of the diodes are kept under the output dc bus voltage and independent of the input voltage. The efficiency of the proposed converter was verified experimentally utilizing a 220-W prototype circuit with an input voltage from 20 to 45 V.

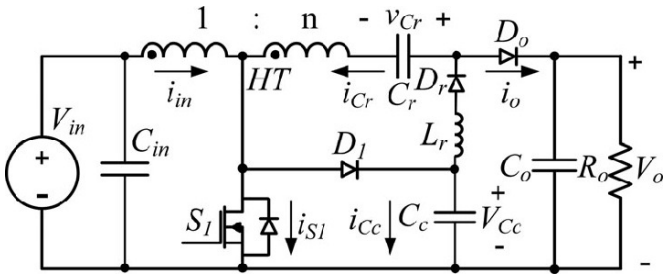

Fig. 3. Proposed high step-up dc–dc converter with hybrid transformer.

II. Proposed Converter Topology and Operation Analysis

Fig. 3 shows the circuit diagram of the proposed converter. C_{in} is the input capacitor; *HT* is the hybrid transformer with the turns ratio 1:*n*; S_1 is the active MOSFET switch; D_1 is the clamping diode, which provides a current path for the leakage inductance of the hybrid transformer when S_1 is OFF, C_c captures the leakage energy from the hybrid transformer and transfers it to the resonant capacitor C_r by means of a resonant circuit composed of C_c , C_r , L_r , and D_r ; L_r is a resonant inductor, which operates in the resonant mode; and D_r is a diode used to provide an unidirectional current flow path for the operation of the resonant portion of the circuit. C_r is a resonant capacitor, which operates in the hybrid mode by having a resonant charge and linear discharge. The turn-on of D_r is determined by the state of the active switch S_1 . D_o is the output diode similar to the traditional coupled-inductor boost converter and C_o is the output capacitor. R_o is the equivalent resistive load.

Fig. 4 illustrates the five steady-state topology stages of the proposed dc–dc converter for one switching cycle. Fig. 5 shows the key voltage and current waveforms for specific components of the converter over the switching cycle. For the waveforms represented in Fig. 5, g_1 represents the driver signal for the active MOSFET switch S_1 ; i_{S1} is the current of the MOSFET S_1 ; i_{Cr} is the current of the resonant capacitor C_r ; i_{Cc} is the current of clamping capacitor C_C ; i_{in} is the primary side current of hybrid transformer; i_o is the current through the output diode; v_{S1} and v_{Do} are the voltage waveforms of the active switch MOSFET S_1 and the output diode D_o , respectively. For simplicity, we assume that the dc input voltage is a stiff voltage source with a constant

voltage V_{in} , the load is a resistor and all the switch and diodes are ideal devices.

The five operation modes are briefly described as follows. [t0 ,t1], [Fig. 3(a)]: In this period, MOSFET S1 is ON, the magnetizing inductor of the hybrid transformer is charged by input voltage, Cr is charged by Cc , and the secondary-reflected input voltage nVin of the hybrid transformer together by the resonant circuit composed of secondary side of the hybrid transformer, Cr , Cc , Lr , and Dr . The energy captured by Cc is transferred to Cr , which in turn is transferred to the load during the off-time of the MOSFET. The current in MOSFET S1 is the sum of the resonant current and linear magnetizing inductor current as shown in Fig. 5. There are two distinctive benefits that can be achieved by the linear and resonant hybrid mode operation. The first benefit is that the energy is delivered from source during the capacitive mode and inductive mode simultaneously. Compared to previous coupled-inductor high boost ratio dc–dc converters with only inductive energy delivery, the dc current bias is greatly reduced, decreasing the size of the magnetics. Second, the turn-off current is decreased, which causes a reduction in the turn-off switching losses. [t1 ,t2], [Fig. 4(b)]: At time t1 , MOSFET S1 is turned OFF, the clamping diode D1 is turned ON by the leakage energy stored in the hybrid transformer during the time period that the MOSFET is ON and the capacitor Cc is charged which causes the voltage on the MOSFET to be clamped.

[t2 ,t3], [Fig. 4(c)]: At time t2 , the capacitor Cc is charged to the point that the output diode Do is forwarded biased. The energy stored in the magnetizing inductor and capacitor Cr is being transferred to the load and the clamp diode D1 continues to conduct while Cc remains charged.

[t3 ,t4], [Fig. 4(d)]: At time t3 , diode D1 is reversed bi-ased and as a result, the energy stored in magnetizing inductor of the hybrid transformer and in capacitor Cr is simultaneously transferred to the load. During the steady-state operation, the charge through capacitor Cr must satisfy charge balance. The key waveform of the capacitor Cr current shows that the ca-pacitor operates at a hybrid-switching mode, i.e., charged in resonant style and discharged in linear style.

[t4 ,t0], [Fig. 4(e)]: The MOSFET S1 is turned ON at time t4 . Due to the leakage effect of the hybrid transformer, the output diode current io will continue to flow for a short time and the output diode Do will be reversed biased at time t0 ; then the next switching cycle starts.

The boost ratio Mb can be obtained by three flux balance crite-ria for the steady state. The first flux balance on the magnetizing inductor of hybrid transformer requires that in steady state

Second, according to flux balance on the resonant inductor during on-time

The last flux balance that governs the circuit is voltage-second balance of the magnetizing inductor in the hybrid transformer for the whole switching period

$$V_{in} D = \frac{V_o - V_{Cr} - V_{in}}{1+n}(1 - D). \quad (3)$$

By substituting (2) into (3), the boost conversion ratio can be obtained

$$M_b = \frac{V_o}{V_{in}} = \frac{n+2}{1-D}. \quad (4)$$

The conversion ratio is similar to the conventional boost converter except that the turns ratio term n is added, so the traditional duty ratio control method that is applied for a standard boost converter can also be applied to the proposed converter.

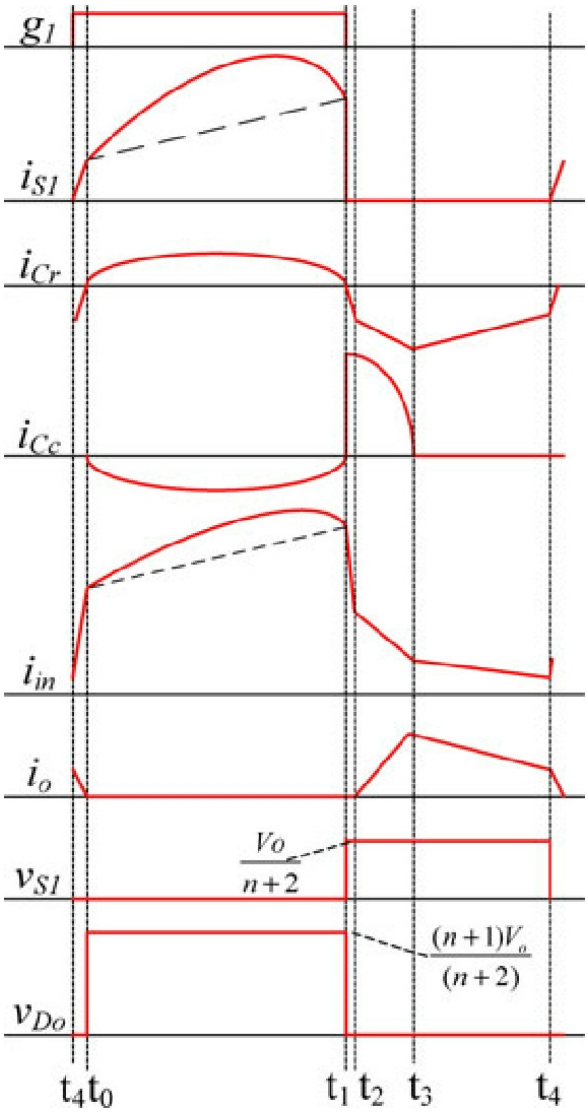

Fig. 5. Key waveforms for different operation stages.

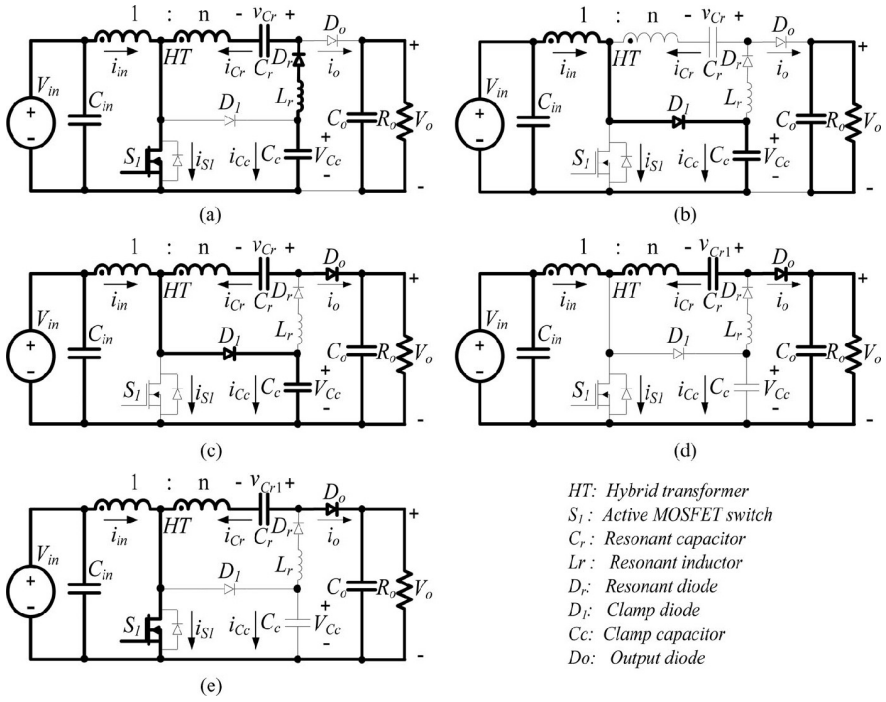

Fig. 4. Operation modes of the high boost ratio dc–dc converter with hybrid transformer. (a) t_0 -t_1 . (b) t_1 -t_2 . (c) t_2 -t_3 . (d) t_3 -t_4 . (e) t_4 -t_5 .

III. Analysis and Advantages of the Proposed Converter

A. Fixed Voltage Stresses of the Power Devices

Proper rating and all the results are with respect to the output dc voltage. From the circuit diagram of t_0 to t_1 and t_1 to t_2 in Fig. 4, respectively, the voltage stresses for MOSFET S_1 and clamping diode D_1 are obtained

$$V_{S_1} = V_{D_1} = \frac{V_{in}}{1-D} = \frac{V_o}{n+2}. \quad (5)$$

From the circuit diagram of t_0 to t_1 and t_2 to t_3 in Fig. 4, one obtains the voltage stress of diode resonant diode D_r and output diode D_o

$$V_{Dr} = V_{Do} = V_o - V_{Cc} = V_o \frac{V_{in}}{1-D} = \frac{(1+n)V_o}{2+n}. \quad (6)$$

From (5) and (6), it is obvious that all the voltage stresses of the switches are independent of input voltage and load conditions. In other words, all the voltage stresses of the switches are optimized based on the output voltage and the turns ratio of the transformer. The resonant period T_r and the resonant frequency are given by

$$T_r = 2\pi\sqrt{L_r C_r} \quad (7)$$

$$f_r = \frac{1}{T_r}. \quad (8)$$

If the constant on-time control T_{on} is used, choose $T_{on} = 1/2T_r$ so that the resonant diode can turn OFF at zero-current condition and conduction loss can be minimized. In the experimental im-plementation of the hybrid transformer, the leakage inductance of the hybrid transformer should be considered, so that the total resonant inductance is expressed as follows

$$L_{r,total} = L_r + L_{lrs} + n^2 L_{lrp} \quad (9)$$

Voltage stresses for all the power devices of the converter are determined in this section to select power devices with the

where L_{lrs} is the secondary side leakage inductance and L_{lrp} is the primary side inductance of the hybrid transformer. The

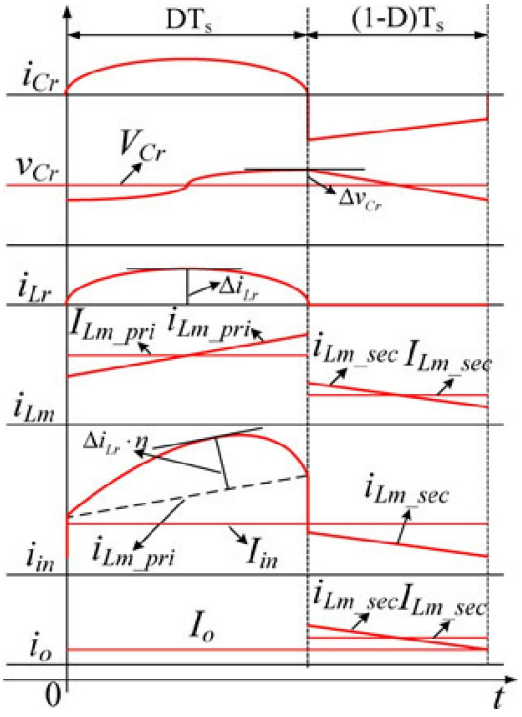

Fig. 6. Waveforms for energy transfer analysis.

resonant capacitance C_r is composed by C_r and C_c in series. Normally, we choose $C_r \gg C_c$ so that the voltage stress of the MOSFET can be clamped well. The optimal operation mode is the constant PWM on-time T_{on} control with variable frequency, however, traditional PWM control method is applicable to the proposed converter as described in [26] and [27].

B. Analysis of Energy Transfer

The simplified waveforms for energy transfer analysis are shown in Fig. 6. In order to analyze the energy transfer feature from the low voltage dc energy source to the high-voltage dc bus, it is necessary to solve the equivalent circuit in Fig. 3(a) subject to the initial conditions imposed by the previous PWM OFF-time interval given by

$$i_{Lr}(0) = 0 \tag{10}$$

$$v_{Cr}(0) = -v_{Cr} \tag{11}$$

where v_{Cr} is the ripple of the resonant capacitor C_r.

The resonant solutions are obtained as

$$i_{Lr}(t) = I_{Lr} \sin 2\pi f_r \cdot t \tag{12}$$

$$v_{Cr}(t) = v_{Cr} \cos 2\pi f_r \cdot t \tag{13}$$

$$v_{Cr} = R_N \cdot I_{Lr} \tag{14}$$

where R_N is characteristic impedance given by

$$R_N = \sqrt{\frac{L_r}{C_r}}. \tag{15}$$

For PWM off-time interval, the discharge equations of the resonant capacitor C_{r1} are given by

$$V_{Cr} = \frac{I_{Lm\_sec} \cdot I_{off}}{2C_r} \tag{16}$$

$$I_{Lm\_sec} = \frac{I_o}{1-D} = \frac{P_o}{V_o} \frac{1}{1-D} \tag{17}$$

where I_{Lm_sec} is the average linear magnetizing current referred to secondary side of the hybrid transformer, I_o is the average output current, P_o is the output power, and V_o is the output voltage.

The relationship between and linear magne-tizing current and sinusoidal resonant current can be expressed as

$$i_{Lr} = \pi \cdot f_r \cdot T_s \cdot I_{Lm\_sec} \cdot (1-D) = \pi \cdot f_r \cdot T_s \cdot I_o. \tag{18}$$

Accordingly, the average primary side sinusoidal resonant current of hybrid transformer is given by

$$L_{Lr\_pri} = \frac{1}{\pi} n \cdot i_{Lr}. \tag{19}$$

Substituting (18) into (19) yields

$$L_{Lr\_pri} = n \cdot f_r \cdot T_s \cdot I_o. \tag{20}$$

The average input current I_{in} can be obtained from (4) by power balance

$$I_{in} = \frac{n+2}{1-D} \cdot I_o. \tag{21}$$

For the optimal mode operation, the relationship between the resonant frequency and the switching period is

$$f_r = \frac{1}{2 \cdot D \cdot T_s}. \tag{22}$$

Substituting (22) into (20) yields

$$L_{Lr\_pri} = \frac{n \cdot I_o}{2D}. \tag{23}$$

The resonant contribution index k_r of energy transfer by sinusoidal resonant current can be defined as the ratio between the average input resonant current I_{Lr_pri} to the total input current I_{in}

$$k_r = \frac{I_{Lr\_pri}}{I_{in}} = \frac{n \cdot I_o}{2D} \Big/ \frac{n+2}{1-D} \cdot I_o = \frac{(1-D)}{2D} \frac{n}{n+2} = \frac{n}{2D} \cdot \frac{V_{in}}{V_o}. \tag{24}$$

In order to optimize the operation of the proposed converter, kr needs to be increased, this will reduce the turn-off losses of the MOSFET and decrease the size of the magnetic core used. The curve of the resonant energy transfer contribution index Kr at different input voltage conditions is shown in Fig. 7. The oper-ating conditions for the curve in Fig. 7 are for when the output voltage Vo equals 400 V, the turns ratio of the hybrid transformer n equals 40:9, and an input voltage range from 20 to 45 V. For a given power and fixed output voltage, the resonant energy trans-fer contribution index increases along with the increase in input voltage. This feature helps improve the converter efficiency over a wide input voltage range by decreasing the conduction losses which are more dominant at low-input voltages and reducing the switching losses that are more dominant at high-input voltages.

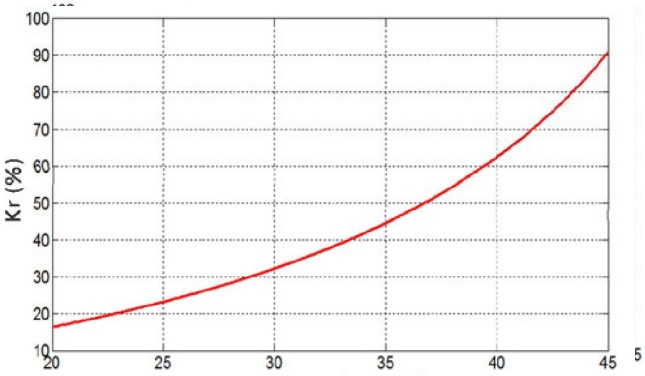

Fig. 7. K_r versus V_{in} curve.

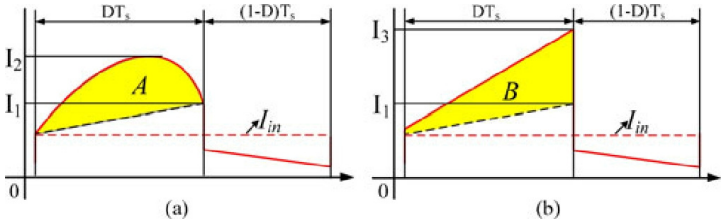

Fig. 8. Input current comparison between resonant mode and linear mode. (a) Resonant mode. (b) Linear mode.

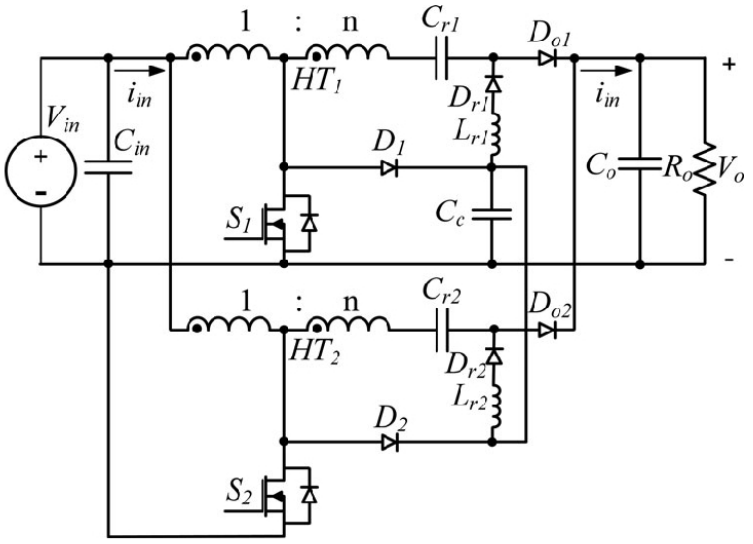

Fig. 9. Two-phase extension for proposed converter.

C. Advantages Over Conventional Nonresonant High Step-Up Converter

Current popular methods used to achieve high boost ratio for nonisolated dc–dc converters consist of using coupled-inductor and switched-capacitor techniques]. The converter presented utilizes hybrid-switching technique combing PWM and resonant power conversions to achieve a high boost ratio while maintaining a high efficiency.

The input currents for the resonant sinusoidal charge mode and the PWM linear charge mode are comparatively illustrated in Fig. 8. The proposed converter works using the resonant sinusoidal charge mode, while a conventional nonresonant converter works using the linear charge mode. For a fixed output power and given input voltage, the average input currents I_{in} for these two converters shown in Fig. 8 are equal. Areas *A* and *B* (see Fig. 8) show the capacitive energy transferred by the hybrid transformer of the proposed converter with resonant mode and linear energy transferred by the coupled-inductor of the converter. The switching losses for a dc–dc converter are directly proportional to the switching current given by the fixed conversion voltages. As shown in Fig. 5, the MOSFET is turned ON at time $t = t_4$, the raising rate of the primary cur-rent is limited by the leakage inductor of the hybrid transformer alleviating the turn-on losses. The main switching loss then becomes the turn-off switching losses. For the resonant mode charge of the proposed converter, the turn-off switching cur-rent I_1 , as shown in Fig. 8(a), consists of only the magnetizing current as a result of resonant operation. For the conventional nonresonant converter ,the turn-off switching current I_3 , as shown in Fig. 8(b), is the sum of the magnetizing current and the switched-capacitor charge current, which is dependent on the leakage inductance of the coupled-inductor. For a given capacitor value of the switched-capacitor, increasing the leakage inductance can reduce the raising rate of the primary side current to reduce the turn-off current; however, the conversion ratio will decrease because of the reduced coupling factor *k* of the coupled-inductor .As a result, the leakage inductance design of the coupled-inductor has a tradeoff between the con-version ratio and a higher turn-off switching current.

With the introduction of a resonant operation mode into the PWM converter for the proposed converter, the primary peak current I_2 , as shown in Fig. 8(b), is smaller than the peak current I_3 of its switched-capacitor counterpart. Since the resonant mode is employed as opposed to the switched-capacitor mode, the

capacitance of the charge capacitor C_r can be greatly reduced. Hence, utilizing the resonant mode allows the use of smaller sized magnetic components and lower profile charge capacitors for C_r which can have a low capacitance. This is perfect for an application where a low profile PV-module-integrated dc– dc converter is needed. The leakage inductance of the hybrid transformer can also be effectively utilized as part of the resonant minor loop simplifying the design of the transformer for the proposed converter.

D. Two-Phase Interleaved Extension

In order for the proposed converter to be used in higher power level conversion applications, the interleaving method applica-ble to the traditional high boost ratio PWM dc–dc converter can be employed, as shown in Fig. 9. This gives the advantages of standard interleaved converter systems such as low-input cur-rent ripple, reduced output voltage ripple, and lower conduction losses. The difference between standard interleaved convert-ers and the proposed interleaved converter is that the clamping capacitor C_c can also be shared by the interleaved units reduc-ing the total number of components in the system. Using the phase-shift method of control, the current ripple through the clamping capacitor C_c is reduced as a result the capacitance needed for C_c is also reduced.

.

V. Conclusion

A high boost ratio dc–dc converter with hybrid transformer suitable for alternative dc energy sources with low dc voltage input is proposed in this paper. The resonant conversion mode is incorporated into a traditional high step-up PWM converter with coupled-inductor and switched-capacitor obtaining the fol-lowing features and benefits:

1) This converter transfers the capacitive and inductive

en-ergy simultaneously to increase the total power delivery reducing losses in the system.

2) The conduction loss in the transformer and MOSFET is re-duced as a result of the low-input RMS current and switch-ing loss is reduced with a lower turn-off current. With these improved performances, the converter can maintain high efficiency under low output power and low-input voltage conditions.

3) With low-input ripple current feature, the converter is suit-able for PV module and fuel cell PCS, where, accurate MPPT is performed by the dc–dc converter.

A prototype-circuit-targeted PV module power optimizer with 20–45 V input voltage range and 400-V dc output was built and tested. Experimental results show that the MOSFET voltage was clamped at 60 V and the output diode voltage was under 350 V. These results were independent of the input voltage level. The conversion efficiencies from 30 to 220 W are higher than 96% and the peak efficiency is 97.4% under 35-V input with 160-W output power.

REFERENCES

[1] J.-S. Lai, "Power conditioning circuit topologies," *IEEE Ind. Electron. Mag.*, vol. 3, no. 2, pp. 24–34, Jun. 2009.

[2] S. B. Kjaer, J. K. Pedersen, and F. Blaabjerg, "A review of single-phase grid-connected inverters for photovoltaic modules," *IEEE Trans. Ind. Appl.*, vol. 41, no. 5, pp. 1292–1306, Sep./Oct. 2005.

[3] F. Blaabjerg, Z. Chen, and S. B. Kjaer, "Power electronics as efficient interface in dispersed power generation systems," *IEEE Trans. Power Electron.*, vol. 19, no. 5, pp. 1184–1194, Sep. 2004.